Appl Biochem Biotechnol (2011) 165:221–234
DOI 10.1007/s12010-011-9245-8

Studies on Silver Accumulation and Nanoparticle Synthesis By *Cochliobolus lunatus*

Rahul B. Salunkhe · Satish V. Patil · Bipinchandra K. Salunke · Chandrashekhar D. Patil · Avinash M. Sonawane

Received: 28 December 2010 / Accepted: 4 April 2011 /
Published online: 20 April 2011

Abstract Development of reliable and eco-friendly processes for synthesis of metallic nanoparticles is an important step in the field of application of nanotechnology. Biological systems provide a useful option to achieve this objective. In this study, potent fungal strain was selectively isolated from soil samples on silver supplemented medium, followed by silver tolerance (100–1,000 ppm) test. The isolated fungus was subjected to morphological, 18S rRNA gene sequencing and phylogenic studies and confirmed as *Cochliobolus lunatus*. The silver accumulation and nanoparticle formation potential of wet cell mass of *C. lunatus* was investigated. The accumulation and nanoparticle formation by wet fungal cell mass with respect to pH change was also studied. The desorbing assay was used to recover accumulated silver from cell mass. *C. lunatus* was found to produce optimum biomass (0.94 g%) at 635 ppm of silver. Atomic absorption spectroscopy study showed that at optimum pH (6.5±0.2), cell mass accumulates 55.6% of 100 ppm silver. SEM and FTIR studies revealed that the cell wall of *C. lunatus* is the site of silver sorption, and certain organic groups such as carbonyl, carboxyl, and secondary amines in the fungal cell wall have an important role in biosorption of silver in nanoform. XRD determined the FCC crystalline nature of silver nanoparticles. TEM analysis established the shape of the silver nanoparticles to be spherical with the presence of very small-sized nanoparticles. Average size of silver nanoparticles (14 nm) was confirmed by particle sizing system. This study reports the synthesis and accumulation of silver nanoparticles through reduction of Ag^{+} ions by the wet cell mass of fungus *C. lunatus*.

R. B. Salunkhe · S. V. Patil · B. K. Salunke · C. D. Patil
School of Life Sciences, North Maharashtra University, Post Box 80, Jalgaon 425001 Maharashtra, India

S. V. Patil (✉)
North Maharashtra Microbial Culture Collection Centre (NMCC), North Maharashtra University,
Post Box 80, Jalgaon 425001 Maharashtra, India
e-mail: satish.patil7@gmail.com

A. M. Sonawane
School of Biotechnology, KIIT University,
Bhubaneswar 751024 Orissa, India

Keywords *Cochliobolus lunatus* · Biosorption · Silver accumulation · Silver nanoparticles

Introduction

Silver released at very high amount to the environment from industrial wastes is estimated at approximately 2,500 tons, of which 150 tons gets into the sludge of wastewater treatment plants and 80 tons is released into surface waters [1, 2]. Microbial cells have the ability to tolerate stressful situations in presence of toxic metals for their survival. The silver tolerating capacity is the result of various specific mechanisms of resistance including efflux systems, altering metal solubility and toxicity, altering redox state of metals, extracellular precipitation of metals, and the inability of metal transport function [3–5]. The tasks like biomineralization, bioaccumulation, bioremediation, bioleaching, microbial corrosion, and very recently microbial fabrication of metal nanoparticles are based on interactions of microorganisms with metals. From an environmental point of view and silver being a precious metal, it is important to remove and recover silver from wastewater like photographic processing waste [6]. Most popular traditional methods such as chemical absorption, oxidation–reduction, and electrolysis were limitedly used because of their technological and economical disadvantages [7–11]. Microorganisms have the potential to become an alternative for silver recovery as they have higher sorption capacity in aqueous solutions [12, 13].

The filamentous fungi possess some distinctive advantages over bacteria in tolerating and absorbing silver. In addition to handling and culturing on a large scale, most fungi have a high tolerance towards metals, and a high wall-binding capacity, as well as intracellular metal uptake capabilities [14]. The fungus *Verticillium*, when exposed to aqueous $AgNO_3$ solution, caused the reduction of the metal ions and formation of AgNPs below the surface of the fungal cells [15]. *Phoma* PT35 was able to selectively accumulate silver [16] and *Phoma* sp. 3.2883 used as biosorbent is suited for preparing silver nanoparticles [17]. *Fusarium oxysporum* [18], *Aspergillus fumigatus*, *Phanerochaete chrysosporium* [19–21], and *Fusarium solani* USM-3799 [22] were able to synthesize silver nanoparticles extracellularly.

The cell wall components of microorganisms have a specific role in absorption and accumulation of metals. The study on mechanism of silver biosorption using dry biomass of *Myxococcus xanthus* showed that silver first binds to cell surface and extracellular polysaccharides and then intracellular deposition occurs [13]. Considering the above facts, it is expected that screening of metal tolerant fungi may provide strains with improved metal sorption capacity and easy metal recovery in nanoform. Only limited studies have been conducted for the isolation and identification of filamentous fungi for their ability of metal tolerance, biosorption potential, and nanoparticle formation.

The fungus *Cochliobolus lunatus* and its conidial anamorphous form *Curvularia lunata* were known for their capacity of hydroxylating β 4–5 steroids [23, 24]. *C. lunatus* is an endophytic fungal plant pathogen and more than 55 species in the genus *Cochliobolus* were identified. However, studies related to silver tolerance are lacking.

In this study, isolation and identification of *C. lunatus* with its potential of silver tolerance, silver biosorption followed by synthesis of silver nanoparticles are reported. Effect of pH on silver sorption by *C. lunatus* was studied. The kinetics of accumulation, site of sorption, biosynthesis, characterization, and mechanism of synthesis of silver nanoparticles were investigated. *C. lunatus* cell mass is an eco-friendly, safe, and reliable approach for silver biosorption and synthesis of silver nanoparticles.

Materials and Methods

Screening and Isolation of Fungi

Soil samples from different sites of Jalgaon district were collected for isolation of the silver tolerating microbes. Soil samples were inoculated in 100 ml sterile enrichment medium. One milliliter of each serially diluted enriched cultures was inoculated in sterile Devis minimal agar medium supplemented with silver (50 ppm) in Petri plates and incubated at 28 °C for 48 h. Different colonies from Devis minimal agar medium containing silver were selected and pure cultures were maintained on potato dextrose agar medium supplemented with $AgNO_3$ having Ag (50 ppm). The isolates were further used for silver tolerance tests.

Silver Tolerance

For the silver tolerance experiment, synthetic Czapek–Dox broth and defined sterile sucrose, peptone, and yeast extract broths were prepared. The final pH was adjusted to 6.5± 0.2. To this, $AgNO_3$ having Ag at concentration ranging from 100 to 1,000 ppm was added separately and inoculated with fungal spores (10^6) of different isolates separately. The flasks were incubated at 28 °C for 24 h in an environmental shaker at 120 rpm in dark condition. The growth of fungal mycelia was observed.

Morphological Characterization, 18S rRNA Gene Sequencing, and Phylogenetic Analysis of the Isolated Fungus

The morphological identification of fungal isolate was determined by bright field microscopy observations of lacto phenol cotton blue stained fungal specimen at 100× magnification.

About 10 mg of fungal mycelia was scraped with a sterile nipper from fresh culture growing on PDA plate at 28 °C for 5–15 days. Fungal DNA was extracted by phenol chloroform method and the primers (NS1 and NS8) and protocols described by White et al. [25] were used to amplify a part of SSU rDNA by polymerase chain reaction (PCR). PCR products were purified using PEG–NaCl method [26] and were bidirectionally sequenced with respective primers using an automated sequencer (3730 DNA analyzer, ABI, Hitachi). Fungal gene sequence generated in this study was aligned with homologous sequences deposited in GenBank using ClustalX (version 2.0.9) [27]. All sequences were manually edited using DAMBE [28]. All uninformative sites were removed from further analysis. Phylogenetic analysis was performed for the dataset and neighbor-joining (NJ) trees were constructed using MEGA 4.1 [29] with 1,000 bootstrap replication and Kimura two-parameter as a model of nucleotide substitution.

Inoculum of Fungi

Inoculum was prepared by using 3% of spore suspension (4×10^6) in sucrose medium incubated at 28 °C for 24 h in an environmental shaker at 120 rpm in dark condition.

Accumulation and Formation of Silver Nanoparticles

C. lunatus was grown in broth containing sucrose, 20 g l^{-1}; peptic digest of animal tissue, 10 g l^{-1}; and yeast extract, 10 g l^{-1}. The final pH was adjusted to 6.5±0.2. The flasks were incubated in the incubator shaker at 28 °C with shaking speed of 120 rpm. After 72 h of

incubation, the mycelial mass was separated by filtration and washed thrice with Milli-Q deionized water. For the washed mycelia, 1 g fresh weight was challenged with 100 ml of silver nitrate solution prepared in Milli-Q deionized water containing Ag at a concentration of 635 ppm and incubated at 28 °C at 120 rpm in dark condition. Simultaneously, controls with mycelial biomass of *C. lunatus* with Milli-Q deionized water and only silver nitrate solution were maintained under the same conditions separately.

Effect of pH on Silver Accumulation

The effect of pH was studied by two types of experiments. In the first experiment, *C. lunatus* was grown in media with pH adjusted in the range of 4.5 to 9.0 and supplemented with Ag (100 ppm) for 72 h at 28 °C. The culture broths were centrifuged at 10,000 rpm for 10 min to separate cell mass. The separated cell mass for each pH was dried at 80 °C; dry mass was weighed, recorded, and the supernatant used for further analysis. In the second experiment, 1 g fresh biomass of *C. lunatus* grown at pH 6.5±0.2 was inoculated in buffer solution having pH ranging from 4.5 to 9.0. The biomass in each flask then challenged with Ag (100 ppm) for 24 h at 28 °C. Accumulation of silver was determined using atomic absorption spectrophotometer (AAS) (Thermo Electron Corp. S series, USA) analysis of filtered supernatants in both experiments.

Silver Desorption Assay

With silver being a precious metal, we recovered absorbed silver by treatment with desorbing agent. Previously challenged dry biomass was suspended in optimized concentration (2 M) of 20 ml ammonia [13] and shaken for 1 h at 120 rpm on a rotary shaker (Remi CIS 24) at 28 °C. The biomass was separated by centrifugation at 5,000 rpm for 10 min and the supernatant was collected. The same procedure was repeated thrice to recover maximum colloidal silver. The desorbate supernatant was filtered through a 0.22-μm filter assembly and used for further analysis.

Characterization of Biosorbed Nanosilver

UV–Visible Spectral Analysis Immediately after incubation of *C. lunatus* biomass with aqueous $AgNO_3$, preliminary detection of AgNPs was carried out by visual observation of color change of the $AgNO_3$ solution. At frequent intervals, filtered supernatant solution and filtered desorbate solution were monitored by sampling 2 ml aqueous part and measuring in the ultraviolet–visible (UV–vis) spectrum monitored on a UV–vis spectrophotometer (Shimadzu 1601 model, Japan) at a resolution of 1 nm from 200 to 800 nm up to 72 h.

Fourier Transform Infrared (FTIR) Analysis To determine the Fourier transform infrared (FTIR) pattern of fungal isolate containing biosorbed nanosilver, FTIR analysis was performed using fine freeze-dried mycelial powder of untreated control and $AgNO_3$ challenged fungal biomass. One gram of sample was mixed with 300 mg of KBr powder and recorded in FTIR (Schimadzu, Japan) at a resolution of 1 cm^{-1}.

X-Ray Diffraction Analysis (XRD) To determine the crystal shape of silver nanoparticles, powder X-ray diffraction was performed using a Phillips PW 1710 X-ray diffractometer with nickel filtered Cu Ka (k=1.54 Å) radiation and analyzed using APD (automatic

powder diffraction) and ORIGIN software. The diffracted intensities were recorded from 20 to 80 2θ angles to obtain the whole spectrum.

Scanning Electron Microscopy (SEM) The freeze-dried mycelial mats (untreated control and silver nitrate treated sample) were mounted on specimen stubs with double-sided adhesive tape and coated with gold in a sputter coater (Bal-Tec SCD-050) and examined under SEM, Philips® XL 30, at 12–15 kV with a tilt angle of 45°.

Transmission Electron Microscopy (TEM) The size and shape of the nanoparticles were observed using a transmission electron microscopy using a Philips Morgagni (268D) operated at an accelerating voltage of 100 kV. A drop of silver nanoparticles solution was placed on a carbon-coated copper grid.

Particle Size Analysis Silver nanoparticles were analyzed on Particle Sizing Systems Inc., USA. The average distribution of nanoparticles on the basis of intensity, volume, and number weighting was studied comparatively.

Results and Discussion

Isolation, Morphological and Molecular Identification, and Phylogenetic Analysis of the Fungal Isolate

From different isolates, the fungi tolerating the highest concentration of silver was selected, identified, and further used for experimentation. Fungal species was identified as *C. lunatus* with morphological identification of colony or hyphal morphology and characteristics of the spores/conidia. Initially, fungal colony on PDA was white colored then turned black; reverse of the colony was yellow to pink. The colony margins were compact and sharply defined. The conidial morphology is boat shaped with four septate owing to the disproportional enlargement at the third cell from the base depending on the isolates or cultural conditions in which they were produced. Spore size of this species was found to range from 18 to 32 μm×8–16 μm (Fig. 1).

The fungal rRNA sequence generated in this study was deposited in GenBank (accession no. HQ731076). The top BLAST match for this sequence was found to be *C. lunatus* (DQ337381) from GenBank with 99% maximum sequence similarity and 100% query coverage. Phylogenetic reconstructions based on alignment of the homologous gene sequences indicated a strong clustering with the sequence from *C. lunatus* (DQ337381) and *Cochliobolus* sp. 007(L)1-1 (FJ235087) which formed a sister clade with different species of *Cochliobolus sativus* and divergent clade with other *Cochliobolus* sp. and *Alternaria* sp. (Fig. 2).

Silver Tolerance of *C. lunatus*

The silver tolerance of *C. lunatus* was tested at concentration ranging from 100 to 1,000 ppm, each assayed at pH 6.5±0.2. The dry biomass (g%) of *C. lunatus* decreased very little and almost linearly with the increasing concentration of silver up to 635 ppm. At 635 ppm, optimum biomass was 0.94 g% in defined medium and 0.78 g% in Czapek–Dox medium, but thereafter the amount of growth slowed down (Fig. 3). To avoid the

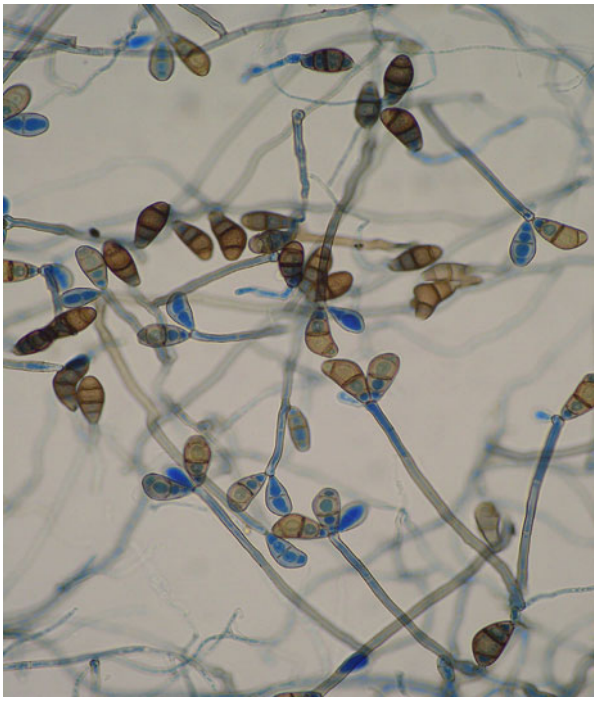

Fig. 1 Bright-field micrograph of boat-shaped characteristic four septate conidial morphology of *Cochliobolus lunatus*

controversy of organic chelation of Ag by medium components and to confirm silver tolerance capacity, fungal growth was also tested in the synthetic medium, Czapek–Dox broth with similar experimental conditions. It was observed that biomass of *C. lunatus* was decreased little in Czapek–Dox broth as compared to defined medium, but silver tolerance capacity remained almost constant (Fig. 3).

Effect of pH

The effect of pH on growth of *C. lunatus* and accumulation and formation of silver nanoparticles was observed at different range of pH. Organism grows well at pH 6.5±0.2

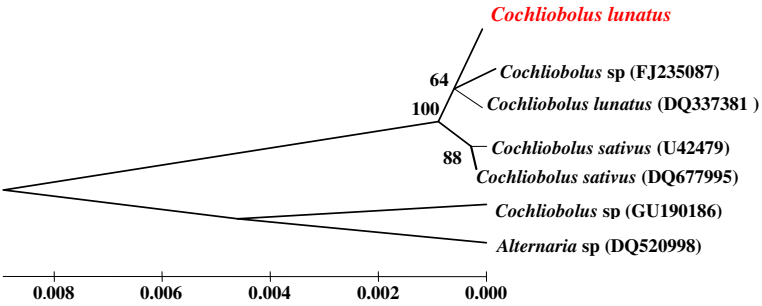

Fig. 2 Phylogenetic relationships between *C. lunatus* from our study (*red*) and those in the GenBank, based on rRNA gene. Levels of confidence for each node are shown in the form of posterior probabilities (PP). Accession numbers are shown after each species name in *parentheses*. *Scale bar* represents substitutions per site

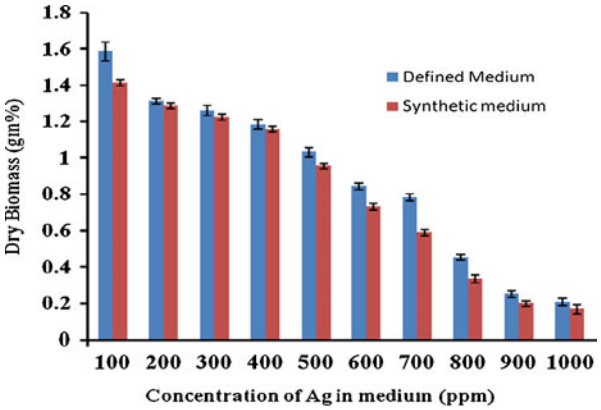

Fig. 3 Silver tolerance capacity of *Cochliobolus lunatus*

with maximum cell mass production, and very less growth was observed at pH 4.5 and pH 9.0. The organism showed high growth and accumulation at pH 6.5±0.2 (data not shown). This observation was further analyzed by challenging cell mass to silver solution at different pH (4.5–9.0). It was observed that the organism accumulates the highest amount of silver at pH 6.5±0.2, i.e., 55.6%, while at pH 4.5 very less silver was accumulated. These results are similar to the previous reports of Kathiresan et al. [30] in which they observed that pH 6.2±0.2 is optimum for nanoparticle formation and accumulation. Comparatively less accumulation at pH 4.5 and 9.0 was found which may be due to silver precipitation at acidic and alkaline pH, respectively (Fig. 4). The accumulation of silver at pH 4.5 was much less than pH 5.5 and pH 9.0, which could be simply due to the competitive inhibition of silver ion accumulation by protons at lower pH. After bioaccumulations of silver, a slight increase in pH values of solutions was observed. This increase could be attributed to ion exchange of H, with Na, K, and other metal ions initially bound in fungal biomass. Parallel results were reported by Zhang et al. [12] using *Aeromonas* sp.

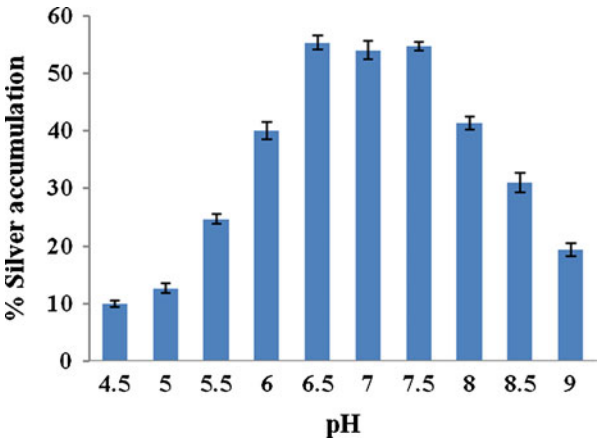

Fig. 4 Effect of pH on silver accumulation by *Cochliobolus lunatus*

Desorption of Silver from Fungal Biomass

The application of fungi as biosorbent depends not only on its biosorptive capacity but also with regeneration of silver and reuse of biomass. The accumulated silver by *C. lunatus* was desorbed using ammonia (2 M) and was found to be converted in nanosize as shown in SEM micrograph (Fig. 7b). These results prove that *C. lunatus* accumulate and converts Ag to nanolevel. The desorbed biomass was processed to reuse it. After reuse, it retains its silver accumulating capacity with a slight decrease than the original (data not shown). Thus, desorbed biomass can be further reused for silver accumulation purpose.

Characterization of Silver Nanoparticles

The surface plasmon resonance is helpful in the determination of optical absorption spectra of metal nanoparticles. Several reports have shown that surface plasmon resonance band of silver nanoparticles occurs at 420 nm [30] and 435 nm [31]. Generally, with the increase in particle size, absorption spectra shift to a longer wavelength [32, 33]. In our case, the UV absorption band occurs at 430 nm. The dispersity, protein core shell of particles, and different shapes and sizes of particles might be responsible for the absorption peaks.

FTIR analysis of biomass of *C. lunatus* before and after silver treatment showed shifting of certain bands and changes in vibration of chemical groups. FTIR measurements of the dried and powdered samples of biomass with AgNPs showed the presence of six intense bands at 1,020.38, 1,091.75, 1,259.56, 1,491.02, 1,747.57, and 2,962.76 cm^{-1} (Table 1). The absorption band at 2,962.76 cm^{-1} corresponds to stretching vibration of secondary amines and the band at 1,743.71 cm^{-1} corresponds to C–O and C=O stretching in carbonyl and carboxyl group in silver untreated biomass. The absorbance band at 2,960.83 cm^{-1} and 1,743.71 cm^{-1} in silver untreated biomass (Fig. 5a) was shifted to 2,962.76 cm^{-1} and 1,747.57 cm^{-1}, respectively, in silver treated biomass (Fig. 5b), which means that these groups positively influence silver. Parallel findings were discussed by researchers [21, 34]. The intense band at 1,462.09 cm^{-1} in Fig. 5a assigned to C=C disappeared after silver treatment (Fig. 5a). In addition, the band at 1,491.02 cm^{-1} assigned to C=N appeared in silver loaded biomass (Fig. 5a). The two bands at 1,020.38 cm^{-1} and 1,369.50 cm^{-1} in Fig. 5a and b showing no change correspond to the C–N stretching vibrations of aliphatic and aromatic amines, respectively. The comparative account of chemical groups involved in biosorption is given in Table 1. The various groups appear or disappear after the formation of Ag and Au nanoparticles; –C=O, –C=C, and –Cl groups appear after Au nanoparticle

Table 1 Comparative peaks in FTIR analysis involved in biosorption of silver

Chemical groups involved in silver biosorption	Peaks before biosorption	Peaks after biosorption	Reference
C–N stretching vibrations of aliphatic and aromatic amine	1,020.38 cm^{-1}	1,020.38 cm^{-1}	[21]
Asymmetrical stretch of ionized carboxyl of amino acids of peptide chains	1,369.50 cm^{-1}	–	[12]
C=C group	1,462.09 cm^{-1}	–	[35]
C=N group	–	1,491.02 cm^{-1}	[35]
C–O and C=O stretching in carbonyl and carboxyl group	1,743.71 cm^{-1}	1,747.57 cm^{-1}	[35]
Stretching vibration of secondary amines	2,960.83 cm^{-1}	2,962.76 cm^{-1}	[21]

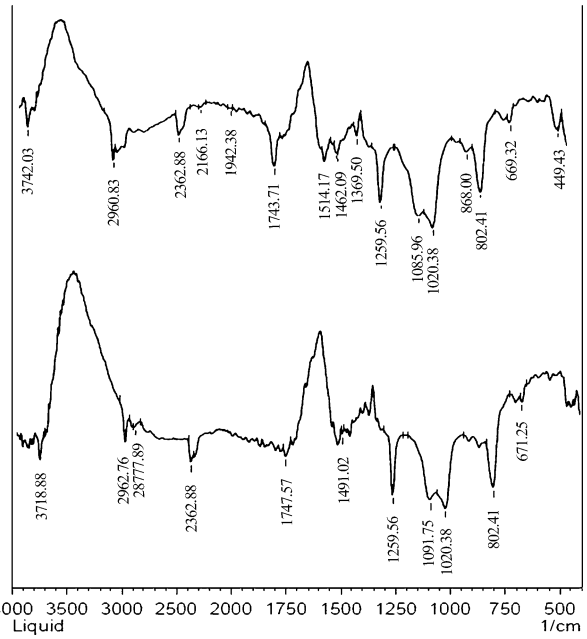

Fig. 5 FTIR spectrum of biomass of *Cochliobolus lunatus* before silver treatment (**a**) and after silver treatment (**b**)

formation was reported [35]. Thus, certain organic groups such as carbonyl, carboxyl, and secondary amines in the fungal cell wall have an important role in biosorption of silver in nanoform. The shifting or group changes after biosorption of metals were discussed by various researchers on the basis of FTIR studies [12, 21].

Further studies using X-ray diffraction were carried out to confirm the crystalline nature of the particles, and the XRD pattern of *C. lunatus* cell mass containing silver is obtained and shown in Fig. 6. The XRD pattern shows four intense peaks at $2\theta°$ values of 38.12, 44.25, 64.42, and 77.50 which corresponds to [111], [200], [220], and [311] planes, respectively. All the four peaks in XRD spectrum agree with the standard report of Joint Committee on Powder Diffraction Standards file no 04-0783. It confirmed that the silver particles formed in our experiments have FCC nanocrystalline nature. The peaks other than nanosilver in XRD analysis (Fig. 6) are due to chitin microfibrils and other groups present in fungal cell wall [21].

The scanning electron micrograph of the fungal biomass untreated control and treated with silver is shown in Fig. 7a, b, respectively. SEM micrograph clearly shows the surface deposited silver nanoparticles (Fig. 7b). The silver nanoparticles have been characterized using SEM by various investigators [12, 17, 18]. The accumulated silver was successfully desorbed using ammonia, and SEM image of desorbate nanosilver (Fig. 7c) confirms that the accumulated silver is converted to nanoform.

Transmission electron microscopy confirmed the morphology and size details of the silver nanoparticles (Fig. 8). A representative typical bright-field TEM micrograph (Fig. 8) shows that AgNPs are symmetrical and spherical shaped, well distributed without aggregation in solution with size ranging from 5 to 100 nm, and with an average size of about 14 nm. The particles are in large numbers, much denser without agglomeration that might be due to protein core shell.

Particle size analysis gives evidence of size and size distribution profile of silver nanoparticles shown in Fig. 9. It revealed that 90% of distribution of particles have small

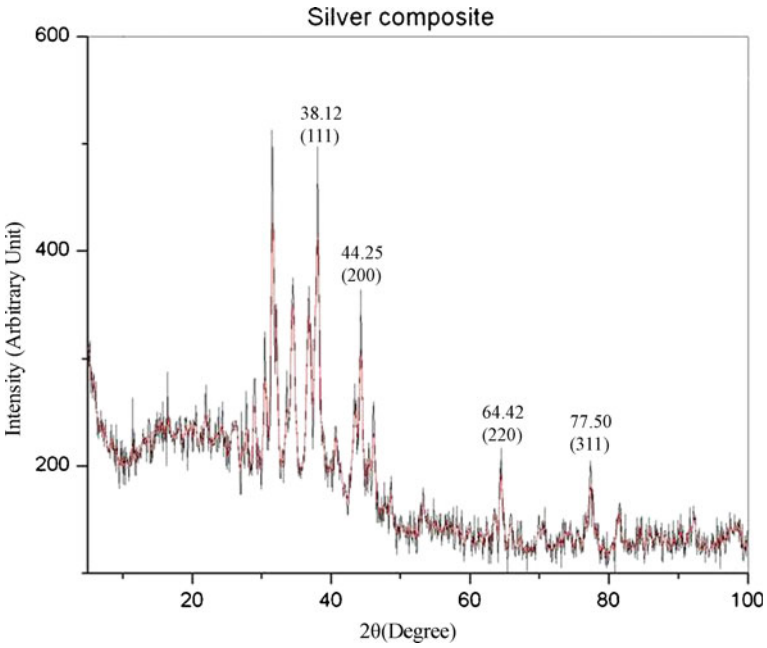

Fig. 6 XRD pattern of *C. lunatus* biomass treated with silver. The XRD pattern shows four intense peaks at $2\theta^{\circ}$ values of 38.12, 44.25, 64.42, and 77.50 which corresponds to [111], [200], [220], and [311] planes, respectively, for silver

(<40 nm) size; thus, the number of smaller particles is more in the sample. The silver nanoparticles have been characterized by various researchers using TEM and particle sizing systems [12, 17, 18].

Mechanism of Silver Nanoparticles Synthesis

There are various mechanisms of biological synthesis described in the literature that are related to NADH-dependent reductases, nitrate reductase [36] oligopeptide catalysis, precipitating the particles with several forms (hexagonal, spherical, and triangular) [37]. The phenomenon of a change in secondary structure of proteins was also reported by reduction of aqueous Ag+ ions using the culture supernatant of *Klebsiella pneumoniae* [38]. However, the fungal reduction of silver ions (Ag+) in aqueous solution generally yields colloidal silver with particle diameter in the range of nanometers. The reduction of various complexes with Ag+ ions leads to the formation of silver atoms (Ag0), which is followed by agglomeration into oligomeric clusters. These clusters eventually lead to the formation of colloidal Ag particles [36].

The nitrate reductase was apparently essential for metal iron reduction but controversially we found 72 h fungal culture negative for nitrate reduction. This result indicates that other mechanisms of Ag reduction may be present. Therefore, in this case, the mechanism of synthesis of AgNPs probably is either by cell wall polymer or by electron shuttle quinones or both.

Fig. 7 SEM analysis of fungal biomass and desorbate: silver untreated biomass (**a**), silver treated biomass (**b**), and desorbed silver (**c**)

a

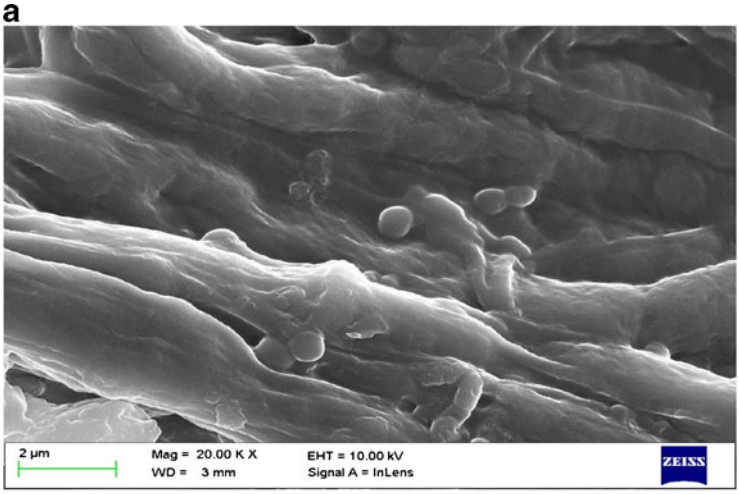
2 µm
Mag = 20.00 K X
WD = 3 mm
EHT = 10.00 kV
Signal A = InLens
ZEISS

b

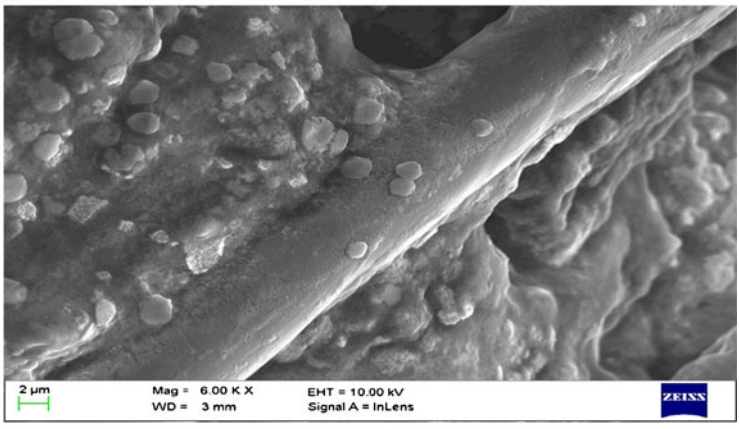
2 µm
Mag = 6.00 K X
WD = 3 mm
EHT = 10.00 kV
Signal A = InLens
ZEISS

c

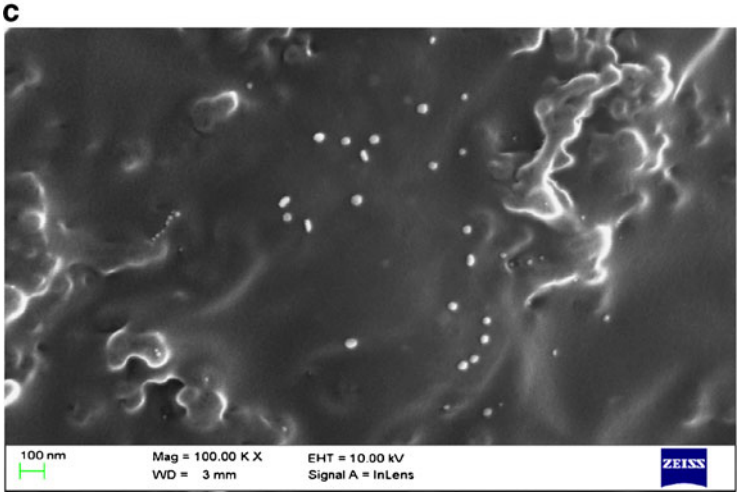
100 nm
Mag = 100.00 K X
WD = 3 mm
EHT = 10.00 kV
Signal A = InLens
ZEISS

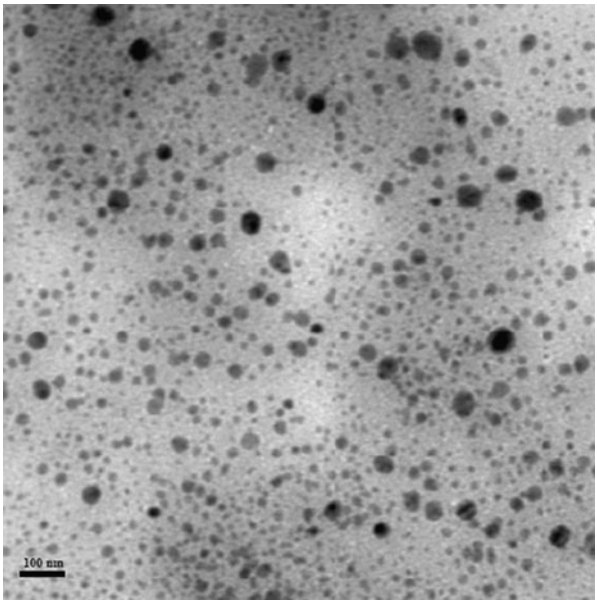

Fig. 8 A representative TEM micrograph of silver nanoparticles recorded from a region of a drop-coated film of silver nitrate solution treated with the cell mass of *C. lunatus* (*scale bar* corresponds to 100 nm)

Besides these extracellular enzymes, NADPH as reducing agent [39], several naphthoquinones [40], and anthroquinones [41] having excellent redox properties were reported in *F. oxysporum* that could act as an electron shuttle in metal reductions [42]. The fungi *C. lunatus* was also reported for production of chochlioquinones [43].

To find out the probable mechanism of silver nanoparticle synthesis using *C. lunatus*, the fungal mass extracted in ethyl acetate was tested by TLC on 250/1 m silica gel GF plates (Hi media GF), using benzene–nitromethane–acetic acid (75:25:2), which resulted in the separation of brown compound detectable at visible light with Rf value of 0.80. The value is in agreement with Rf value of quinones produced by *Fusarium* sp. [44]. This will lead to

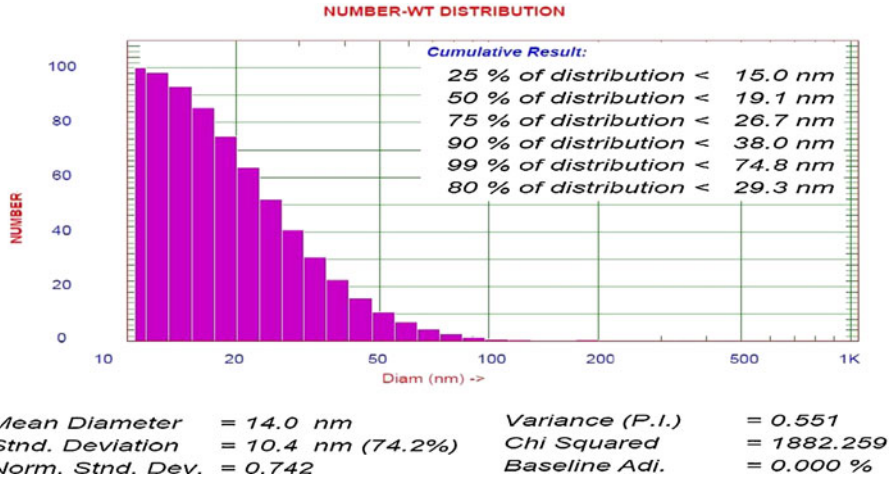

Fig. 9 The particle size distribution histogram of silver nanoparticles obtained using a Particle Sizing Systems Inc., USA shows size distribution of silver nanoparticles

the possibility that quinones may have a certain role along with cell wall composition in reduction of silver to nanoform as several naphthoquinones and anthraquinones having very high redox potentials have been reported from *F. oxysporum* that could act as an electron shuttle in metal reduction [42].

Conclusion

The use of *C. lunatus* cell mass for accumulation of silver and subsequent formation of silver nanoparticles is a promising new approach to develop technology. This top-down approach of biological synthesis has advantages over other methods as it ensures tremendous specificity in the formation of silver nanoparticles, their size, shape, uniform crystallographic orientation, monodispersity, and of course maximum stability.

Acknowledgment We would like to express our gratitude to Dr. N. Vigneshwaran, Sr. Scientist, CIRCOT, Mumbai for his useful advice and support and Prof. P. P. Patil, Director, School of Physical Sciences, North Maharashtra University, Jalgaon for analytical improvement of manuscript and encouragement.

References

1. Smith, I. C., & Carson, B. L. (1977). *Trace metals in the environment, vol 2—silver*. Ann Arbor: Ann Arbor Science.
2. Petering, H. G. (1984). Silber. In E. Merian (Ed.), *Metalle in derUmwelt, Verteilung, Analytik und biologische Relevanz* (pp. 555–560). Weinheim: Verlag.
3. Rouch, D. A., Lee, B. T., & Morby, A. P. (1995). *Journal of Industrial Microbiology, 14*, 132–141.
4. Silver, S. (1996). *Gene, 179*, 9–19.
5. Beveridge, J. T., Hughes, M. N., Lee, H. K. T., Poole, R. K., Savvaidis, I., Silver, S., et al. (1997). *Advances in Microbial Physiology, 38*, 178–243.
6. Pethkar, A. V., & Paknikar, K. M. (2003). *Process Biochemistry, 38*, 855–860.
7. Chen, J. P., & Lim, L. L. (2002). *Chemosphere, 49*, 363–370.
8. Pollet, B., Lorimer, J. P., Phull, S. S., & Hihn, J. Y. (2000). *Ultrasonics Sonochemistry, 7*(2), 69.
9. Ajiwe, V. I. E., & Anyadiegwu, I. E. (2000). *Separation and Purification Technology, 18*, 89–92.
10. Adani, K. G., Barley, R. W., & Pascoe, R. D. (2005). *Mineral Engineering, 18*, 1269–1276.
11. Othman, N., Mat, H., & Goto, M. (2006). *Journal of Membrane Science, 282*, 171–177.
12. Zhang, H., Li, Q., Wang, H., Sun, D., Lu, Y., & He, N. (2007). *Applied Biochemistry and Biotechnology, 143*, 54–62. doi:10.1007/s12010-007-8006-1.
13. Merroun, M. L., BenOmar, N., Alonso, E., Arias, J. M., & Gonzalez-Munoz, M. T. (2001). *Geomicrobiology, 18*, 183–192.
14. Dias, M. A., Lacerda, I. C. A., Pimentel, P. F., DeCastro, H. F., & Rosa, C. A. (2002). *Letters in Applied Microbiology, 34*, 46–50.
15. Mukherjee, P., Ahmad, A., Mandal, D., Senapati, S., Sainkar, S. R., Khan, M. I., et al. (2001). *Angewandte Chemie. International Edition, 40*, 3585–3588.
16. Pighi, L., Pumpel, T., & Schinner, F. (1989). *Biotechnology Letters, 11*, 275–280.
17. Chen, J. C., Lin, Z. H., & Ma, X. X. (2003). *Letters in Applied Microbiology, 37*, 105–108.
18. Ahmad, A., Mukherjee, P., Senapati, S., Mandal, D., Khan, M. I., Kumar, R., et al. (2003). *Colloids and Surfaces. B: Biointerfaces, 28*, 313.
19. Bhainsa, K. C., & D'Souza, S. F. (2006). *Colloids and Surfaces. B: Biointerfaces, 47*, 160–164.
20. Vigneshwaran, N., Kathe, A. A., Varadrajan, P. V., Nachane, R. P., & Balasubramanya, R. H. (2006). *Collides & Surfaces B: Biointerfaces, 53*, 55–59.
21. Vigneshwaran, N., Ashtaputre, N. M., Varadarajan, P. V., Nachane, R. P., Paralikar, K. M., & Balasubramanya, R. H. (2007). *Materials Letters, 61*, 1413–1418.

22. Ingle, A., Rai, M., Gade, A., & Bawaskar, M. (2008). *Journal of Nanoparticle Research*. doi:10.1007/s11051-008-9573-y.
23. Vitas, M., Smith, K., Rozman, D., & Komel, R. (1994). *Journal of Steroid Biochemistry and Molecular Biology, 49*, 87–92.
24. Padua, R. M., Oliveira, A. B., Filho, J. D., Takahashi, J. A., Silva, M. A., & Braga, F. C. (2007). *Journal of the Brazilian Chemical Society, 18*(7), 1303–1310.
25. White, T. J., Bruns, T., Lee, S., & Talor, J. (1990). Amplification and direct sequencing of fungal ribosomal RNA genes for phylogenetics. In: *PCR protocols: a guide to methods and applications*, (pp. 315–322). San Diego: Academic.
26. Sambrook, J., Fritsch, E. F., & Maniatis, T. (1989). *Molecular cloning: a laboratory manual* (2nd ed.). Cold Spring Harbor: Cold Spring Harbor Laboratory Press.
27. Larkin, M. A., Blackshields, G., Brown, N. P., Chenna, R., McGettigan, P. A., McWilliam, H., et al. (2007). *Bioinformatics, 23*, 2947–2948.
28. Xia, X., & Xie, Z. (2001). *The Journal of Heredity, 92*, 371–373.
29. Tamura, K., Dudley, J., Nei, M., & Kumar, S. (2007). MEGA4: molecular evolutionary genetics analysis (MEGA) software version 4.0. *Molecular Biology and Evolution, 24*, 1596–1599.
30. Kathiresan, K., Manivannan, S., Nabeel, M. A., & Dhivya, B. (2009). *Colloids and Surfaces. B: Biointerfaces, 71*, 133–137.
31. Vigneshwaran, N., Kathe, A. A., Varadrajan, P. V., Nachane, R. P., & Balasubramanya, R. H. (2007). *Langmuir, 23*, 7113–7117.
32. Morones, J. R., Elechiguerra, J. L., Camacho, A., & Ramirez, J. T. (2005). *Nanotechnology, 16*, 2346–2353.
33. Pal, S., Tak, Y. K., & Song, J. M. (2007). *Applied and Environmental Microbiology, 27*(6), 1712–1720.
34. Pethkar, A. V., Kulkarni, S. K., & Paknikar, K. M. (2000). *Bioresource Technology, 80*, 211–215.
35. Singh, A. K., Talat, M., Singh, D. P., & Srivastava, O. N. (2010). *Journal of Nanoparticle Research, 12*, 1667–1675.
36. Vaidyanathan, R., Shubaash, G., Kalimuthu, K., Venkataraman, D., Sureshbabu, R. K. P., & Sangiliyandi, G. (2009). *Colloids and Surfaces B: Biointerfaces*. doi:10.1016/j.colsurfb.2009.09.006.
37. Naik, R. R., Stringer, S. J., Agarwal, G., Jones, S. E., & Stone, M. O. (2002). *Nature Materials, 1*, 169–172.
38. Shahverdi, A. R., Fakhimi, A., Shahverdi, H. R., & Minaian, S. (2007). *Nanomedicine: Nanotechnology, Biology, and Medicine*. doi:10.1016/j.nano.2007.02.001.
39. Duran, N., Marcato, P. D., Alves, O. L., De Souza, G. H., Esposito, E. (2005). *Journal of Nanobiotechnology 3*, 8.
40. Bell, A. A., Wheeler, M. H., Liu, J. G., & Stipanovic, R. D. (2003). *Pest Management Science, 59*, 736–747.
41. Baker, R. A., & Tatum, J. H. (1998). *Journal of Fermentation and Bioengineering, 85*, 359–361.
42. Newman, D. K., & Kolter, R. (2000). *Nature, 405*, 94–97.
43. Campos, F. F., Rosa, L. H., Cota, B. B., Caligiorne, R. B., Rabello, A. L., Almeida Alves, T. L., et al. (2008). *PLOS Neglected Tropical Diseases, 2*(12), e348.
44. Medentsev, A. G., & Alimenko, V. K. (1998). *Phytochemistry, 47*, 935–959.